RESEARCH ARTICLE

Synthesis and Characterization of Three-Dimensional Mesoporous Cerium Oxide Hollow Sphere and its Application as Efficient Electrochemical Sensor for Determination of Terazosin

Najmeh Farvardin[1], Shohreh Jahani[2], Maryam Kazemipour[1], Mohammad Mehdi Foroughi[1,]*

[1] *Department of Chemistry, Kerman Branch, Islamic Azad University, Kerman, Iran*

[2] *Noncommunicable Diseases Research Center, Bam University of Medical Sciences, Bam, Iran*

ARTICLE INFO

Article History:
Received 2021-06-27
Accepted 2021-11-01
Published 2022-06-30

Keywords:
Cerium oxide,
Terazosin,
Mesoporous,
Nanostructure,
Voltammetry.

ABSTRACT

Three-dimensional mesoporous CeO_2 hollow sphere (M-CeO_2-HS) modified by glassy carbon electrode (M-CeO_2-HS/GCE) is developed in this study as a very sensitive voltammetric sensor for detection of terazosin. This produced modifier is characterized by techniques, including X-ray diffraction (XRD), scanning electron microscopy (SEM) and energy dispersive X-ray spectroscopy (EDS). There is a remarkable improvement in the electrochemical behavior relative to terazosin electro-oxidation on M-CeO_2-HS/GCE surface, compared to bare GCE, in the optimized conditions of supporting electrolyte pH and casted modifier concentration. An oxidation peak was found for terazosin on modified electrode surface at the potential of about 0.57 V in phosphate buffer solution (pH=7.0). The linear dynamic range was 0.01 to 600.0 µM and the limit of detection was 1.9 nM with the aid of anodic peak of terazosin. Some advantages are reported for the modified electrode, including satisfactory reproducibility towards terazosin, potent stability, strong sensitivity and easy production. Practical application of the M-CeO_2-HS/GCE was tested to detect the low level of terazosin in clinical and pharmaceutical formulations.

How to cite this article
Farvardin N., Jahani S., Kazemipour M., Foroughi M. M. Synthesis and Characterization of Three-Dimensional Mesoporous Cerium Oxide Hollow Sphere and its Application as Efficient Electrochemical Sensor for Determination of Terazosin. J. Nanoanalysis., 2022; 9(2): 137-147. DOI: 10.22034/jna.2021.1934201.1263.

INTRODUCTION

Terazosin has been shown to be a potent, selective adreno-receptor antagonist and acts as a strong drug in the management of hypertension [1, 2] through the vein and arterial relaxation and in the symptomatical management of urinary obstruction following benign prostatic hyperplasia (BPH) through the prostate and bladder muscular relaxation. The adsorption of oral terazosin is complete and fast from the gastrointestinal tract, with the bioavailability of 90%. The metabolism of terazosin is mainly in the liver, and its excretion occurs through the biliary tract [3-6]. Intravenous and oral terazosin have been detected in bulk form, biological fluids and pharmaceuticals using various analytical techniques, including spectrophotometry, spectrofluorimetry, HPLC, voltammetric method, HPLC with UV detector and with fluorescence detector, normal phase HPLC electrospray mass spectroscopy and HPLC with photodiode array detector [7-14].

Industrial process control, medicine and biotechnology, and environmental monitoring can be achieved by electrochemical techniques [15-23]. There is interesting attention towards chemically modified electrodes (CMEs) to analyze various materials at trace level by sensitive electroanalytical methods because of selecting simple modifier for each analyte owing to high selectivity and sensitivity of electroanalytical response based on modifier features. The advantages of electrodes modified with metal oxides are wide potential window, potent stability and catalytic ability [24–

* Corresponding Author Email: *foroughi@iauk.ac.ir*

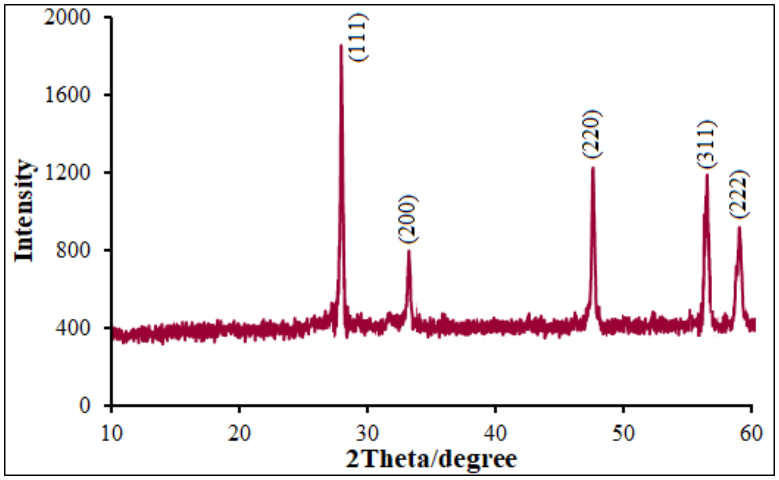

Fig. 1. XRD pattern of mesoporous CeO_2 hollow spheres.

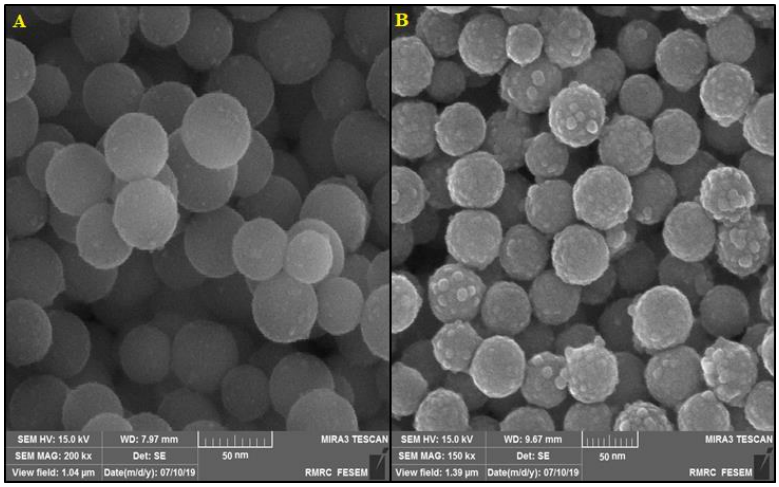

Fig. 2. FESEM image of (A) SiO_2 nanoparticles, (B) mesoporous CeO_2 hollow spheres.

28]. Recently nanoparticles are used in many fields [29-35].

Cerium oxide (CeO_2) as an abundant catalytic material is a low toxic and cost-effective, stable n-type semiconductor, thereby CeO_2-based substances as promising catalysts in the electrochemical process. According to our previous findings, the ordered mesoporous CeO_2 with large surface area had greater catalytic activity when comparing to conventional CeO_2 as the regular compound. The nanomaterials reduce the over potential of redox reaction of electroactive species because of the large surface to volume ratio [36-38]. The nanomaterials can be applied as modifiers in GCEs.

In our recent study, a hydrothermal approach was introduced to construct three-dimensional mesoporous CeO_2 hollow sphere (M-CeO_2-HS). The unique merits found for M-CeO_2-HS guide us to use this case for the GCE surface modification in the fabrication of effective electrochemical sensors. The present study aimed to detect terazosin by designing an easy method capable of modifying the GCE surface using M-CeO_2-HS (M-CeO_2-HS/GCE) exploiting electrochemical tests to determine several analytical parameters.

EXPERIMENTS

Chemicals and reagents

Sigma-Aldrich was the selected company to prepare cerium nitrate hexahydrate, ammonium hydroxide, ethylene glycol, tetraethylorthosilcate and NaOH. The preparation of fresh terazosin stock solutions was performed in PB (0.1 M phosphate

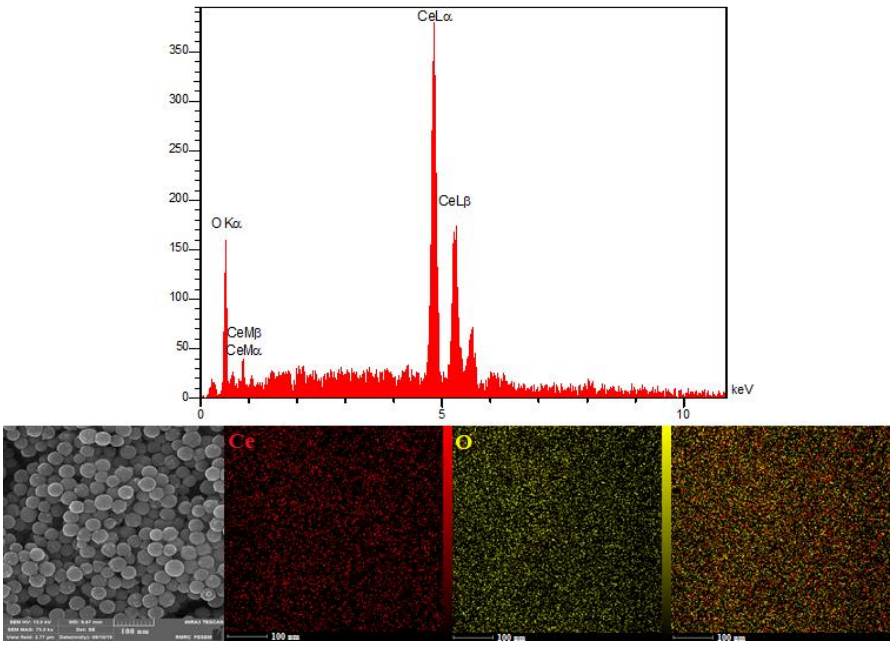

Fig. 3. EDX spectra and elemental mapping of mesoporous CeO_2 hollow spheres.

buffer pH=7.0). All electrochemical tests were carried out by 0.1 M KCl solution having 5 mM $[Fe(CN)_6]^{-3/-4}$ as Redox probe. Deionized water (DW) was applied to prepare all aqueous solutions.

Instrument

Philips analytical PC-APD X-ray diffractometers with graphite monochromatic Cu radiation (α_1, λ_1=1.54056 Å) and Kα radiation (α_2, λ_2=1.54439 Å) were employed to determine the products of the organization. The M-CeO_2-HS was characterized by scanning electron microscope (SEM) and energy dispersive X-ray spectroscopy (EDS or EDX, EM 3200 and KYKY). Cyclic voltammetry (CV), differential pulse voltammetry (DPV), electrochemical impedance spectroscopy and chronoamperometry were implemented on a three-electrode-system (SAMA 500 Electro analyzer) consisting of Ag/AgCl (reference electrode), glassy carbon (working electrode), and platinum (counter electrode). The pH values were measured by a pHS-3C pH meter (Shanghai REX Instrument Factory, China). All tests were performed at an ambient temperature of 25°C.

Construction of 3D M-CeO_2-HS

For this purpose, first a mix of tetraethylorthosilcate (8 mL) and ethanol (280 mL) and then 8.4 mL of ammonium hydroxide and 56 mL of deionized water were transferred into a flask and stirred with a high speed rate at a room temperature overnight, followed by collecting the products after centrifugation at 8500 rpm, dried at 60°C for 6 hours. Next, the dried SiO_2 (100 mg) was ultra-sonicated in ethylene glycol (13 mL), and subsequently added by deionized water (0.75 mL) and cerium nitrate hexahydrate (0.5 g), stirred for 30 minutes for homogenization, autoclaved and heated in the oven at a temperature of 120°C for 24 hours. The air-cooled product was centrifuged at 10000 rpm to gather SiO_2@CeO_2 particles, which were washed by absolute ethanol and dispersed in 5mol/l NaOH for two days to collect M-CeO_2-HS for next testing [26].

Construction of M-CeO_2-HS/GCE

Prior to modification, the bare GCE was polished by different concentrations of alumina slurries (1.0, 0.3, and 0.05 μm) and washed in an ultrasonic bath for 3 minutes successively with ethanol and distilled water, and dried in nitrogen (N_2) and blown prior to analysis. In addition, M-CeO_2-HS powder (1 mg) was dissolved in DW (1 mL) for 30 minutes under ultra-sonication to prepare a suspension. Then, the suspension (5 μl) was added drop wise to the pre-polished GCE surface and dried at 60°C for 20 minutes. The

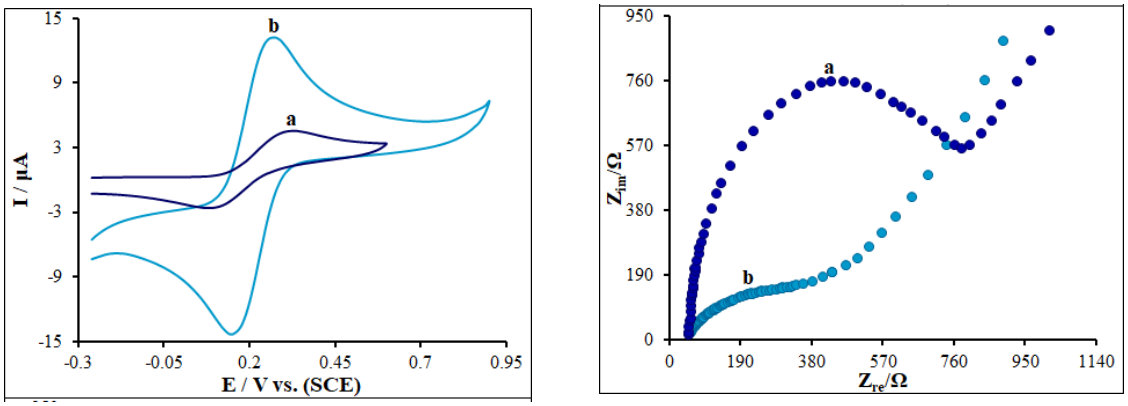

Fig. 4. (A) CVs of (a) unmodified GCE and (b) M-CeO_2-HS/GCE in the presence of 0.5 mM $[Fe(CN)_6]^{3-}$ solution in aqueous 0.1 M KCl the scan rate was 50 mV s^{-1}. (B) EIS diagrams for 0.5 mM $[Fe(CN)_6]^{3-}$ solution at (a) unmodified GCE and (b) M-CeO_2-HS/GCE in aqueous 0.1 M KCl. Frequency range 100 KHz to 0.1 Hz.

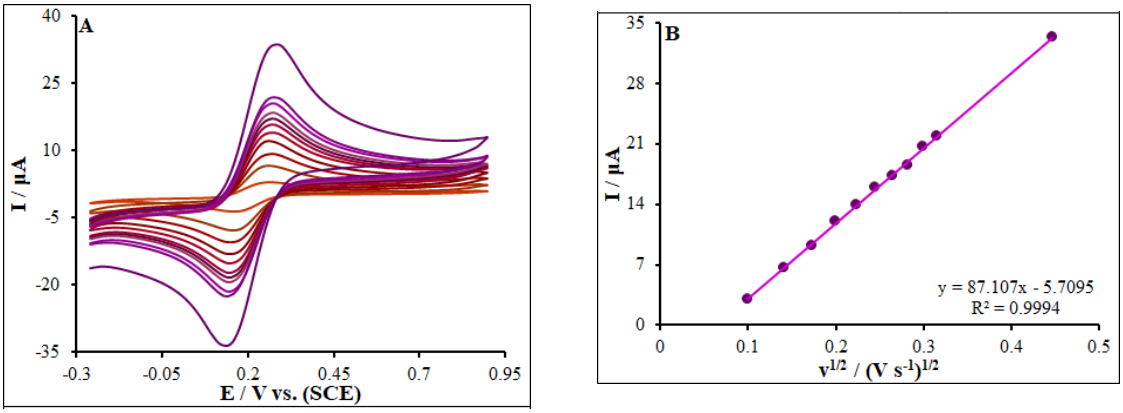

Fig. 5. (A) CVs of M-CeO_2-HS/GCE in the presence of 0.5 mM $[Fe(CN)_6]^{3-}$ solution in aqueous 0.1 M KCl at various scan rates (from inner to outer curve): 10, 20, 30, 40, 50, 60, 70, 80, 90, 100 and 200 mV/s. (B) The plot of peak currents vs. $v^{1/2}$.

M-CeO_2-HS-modified GCE (M-CeO_2-HS/GCE) was utilized for terazosin detection.

Analysis of real specimens

We procured the tablet solutions by completely powdering and combining 5 terazosin tablets (labeled 2 mg, Hakim Co., Tehran: Iran). Then, we used the ultrasonic bath for four minutes in order to dissolve a sufficient volume of the resulting fine powders of terazosin in 0.1 M phosphate buffer pH=7.0. Consequently, various volumes of all solutions have been transferred into a 25.0 mL voltammetric cell and standard addition procedure has been used to analyze terazosin.

The human samples (urine and blood serum) were collected from healthy subjects and stored at -20°C for next testing. In the experiments, 2.5 ml of samples were poured into PB (22.5 ml)-containing vials, and then added with certain volume of terazosin stock solution and subsequently poured into electrochemical cells.

RESULTS AND DISCUSSION

Characterization of M-CeO_2-HS surface

The XRD spectrum (Fig. 1) was obtained for the M-CeO_2-HS to analyze the crystalline steps and calculate the crystallite dimensions using Scherrer's equation. The results showed an overall characteristic between 10° and 60° (2θ) regarding the normal reflection of CeO_2 phase (PDF#04-0593) related peak 111 at about 28.6° [36]. The mean crystalline size was estimated at about 48 nm for CeO_2. The XRD peaks of each pattern for the cubic fluorite structure of CeO_2 included (111), (200), (220), (311) and (222) planes (Fig. 1) [37, 38]. There were no SiO_2 diffraction peaks in the XRD pattern of CeO_2 nanostructures, which means complete removal of SiO_2 from the product.

Table 1. Comparison of the efficiency of different methods used in detection of terazosin.

Method	Modifier	LOD	LDR (μM)	Ref
Voltammetry	Palladium nanoparticle film	19.0 nM	0.01-1000.0	[42]
Voltammetry	Sodium dodecyl sulfate	0.6 μM	0.04-2.4	[43]
Voltammetry	ZnO nanoparticles and reduced graphene oxide	2.0 nM	1.0-10.0	[44]
Voltammetry	Poly congo red	7.3 μM	17.6-33.3	[45]
Voltammetry	M-CeO_2-HS/GCE	1.9 nM	0.01-600.0	This work

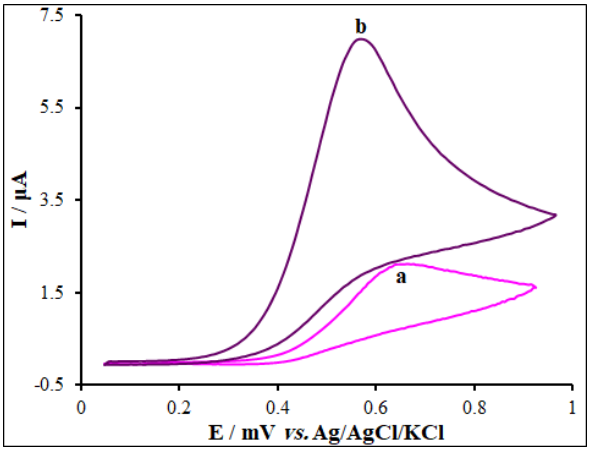

Fig. 6. CVs of a) unmodified GCE and b) M-CeO_2-HS/GCE in 0.1 M PBS (pH 7.0) containing terazosin (75.0 μM). In all cases, the scan rate was 50 mV s^{-1}.

The magnitude of the particle size was calculated by the Debye-Scherrer equation, equation 1, [39, 40].

$$D=0.9\lambda/\beta\cos\theta \quad (1)$$

Where λ is the wavelength of the peak, β is the peak width at half of the relevant peak, θ is Bragg angle and D is average crystalline size. According to Debye-Scherrer equation the average crystallite size (d) of it was calculated about 30.0 nm.

The particle morphology of SiO_2 is spherical according to Fig. 2a and the M-CeO_2-HS possess fine CeO_2 particles as seen in Fig. 2b. The CeO_2 nanoparticles were mounted in a uniform manner on the SiO_2 surface to develop three-dimensional hollow sphere configuration, with the diameter of hollow spheres of about 49 nm.

Based on Fig. 3, the CeO_2 hollow sphere was verified using the EDX mapping images, which showed the hollow core containing Ce and O elements.

Electrochemical characterization of M-CeO_2-HS/GCE sensor

The CV curves for bare GCE and M-CeO_2-HS/GCE in the redox probe were plotted for the characterization of modified GCE surface. As seen in Fig. 4a, two reversible redox peaks are observed for M-CeO_2-HS/GCE versus GCE, with a peak-to-peak difference (ΔEp) of 0.23 V and 0.11 V, respectively. The M-CeO_2-HS/GCE had an enhancement in the peak current corresponding to greater porosity of M-CeO_2-HS-modified electrode surface. The redox probe electron transfer on the modified electrode surface can be facilitated by such excellent morphology of the M-CeO_2-HS/GCE. The properties of M-CeO_2-HS/GCE were electrochemically determined using the EIS approach. In this method, the charge–transfer resistance (Rct) is a factor to monitor the redox probe electron transfer kinetics at the electrode interface, which means substrate attachment on modified electrode surface. Fig. 4b shows the Nyquist plots of M-CeO_2-HS/GCE and GCE in

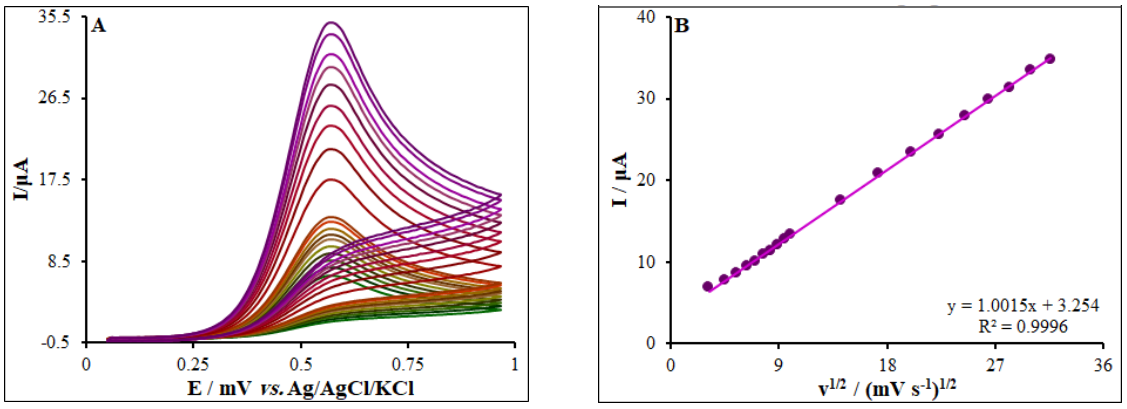

Fig. 7. (A) CVs of M-CeO_2-HS/GCE in pH 7.0 in the presence of terazosin (125.0 µM) at various scan rates (from inner to outer curve): 10, 20, 30, 40, 50, 60, 70, 80, 90, 100, 200, 300, 400, 500, 600, 700, 800, 900 and 1000 mV/s. (B) The plots of peak currents vs. $\upsilon^{1/2}$.

the redox probe and a large semicircular part for bare GCE at high frequencies, as a great charge transfer resistance (Rct=1069 Ω) corresponding to low charge and mass transfer rate on the bare GCE surface. Dramatically reduced Rct (284 KΩ) was calculated for M-CeO_2-HS loaded on GCE surface, probably due to the potent ability of M-CeO_2-HS to amplify the electron transfer and enhance the electrode surface area.

The Randles–Sevcik Equation (2) was computed to analyze the efficacy of embedded sensor, the GCE and M-CeO_2-HS/GCE (Fig. 5) [41]:

$$I_p = \pm (2.69\times10^5)\, n^{3/2}\, A\, D^{1/2}\, C\, v^{1/2} \qquad (2)$$

Where, all symbols possess normal meaning. The A values are 0.23 and 0.078 and cm^2 for the surfaces of M-CeO_2-HS/GCE and GCE, respectively. The special properties of M-CeO_2-HS are in accordance with the 2.9-fold A value of M-CeO_2-HS/GCE surface that means their ability to provide greater surface area and to amplify the current signal.

The electrode surface modification was evaluated by calculating standard heterogeneous rate constant (k^0) based on the EIS, Equation (3), [41]:

$$k^0 = \frac{RT}{F^2 R_{ct} A C} \qquad (3)$$

Where, k^0 stands for rate constant for electron standard transfer that is heterogeneous (cm/s), R for global gas constant (squared with 8.314 J/K/mol), T for temperature of thermodynamic process (298.15 K), F for the Faraday constant values (96.485 C/mol), R_{ct} for electron transfer resistance (Ω), A for electrode surface area (cm^2) and C for concentration of 0.1 mM $[Fe(CN)_6]^{3-/4-}$ solution.

The k^0 values were 4.1×10^{-2} and 3.2×10^{-2} cm/s for M-CeO_2-HS/GCE and GCE, respectively. K^0 values approach the redox couple's kinetic potential. Therefore, a system with a higher value of k^0 balances under lower time conditions compared with a lower value of k^0, so this will be a longer balance. Hence, higher value of k^0 would be achieved M-CeO_2-HS/GCE>GCE as for M-CeO_2-HS/GCE sensor, which means greater swift electron transfers in comparison to the other electrodes.

Electrochemical profile of terazosin on M-CeO_2-HS/GCE surface

The CVs obtained from bare GCE and M-CeO_2-HS/GCE in 0.1 M PBS at the pH value of 7.0 are seen in Fig. 6. The oxidation peak was at 650 mV (curve a) for 75.0 µM terazosin in PB on bare electrode (Fig. 6). When comparing with bare GCE, the peak potential switched to 570 mV (curve b) positively, with a sharper oxidation peak on M-CeO_2-HS/GCE. There was also approximately 3.2-fold elevation in the peak current for M-CeO_2-HS/GCE (curve b) when comparing with bare GCE. The findings verified successful load of M-CeO_2-HS on electrode, which could detect terazosin and confirmed the electrode sensitivity.

The scan rate effect

Fig. 7 shows CVs for 125.0 µM terazosin at different scan rates on M-CeO_2-HS/GCE. A gradual increase was observed in the peak currents of terazosin oxidation by elevating scan rates from 10 to 1000 mV/s, as seen in Fig. 7. Terazosin Ipa

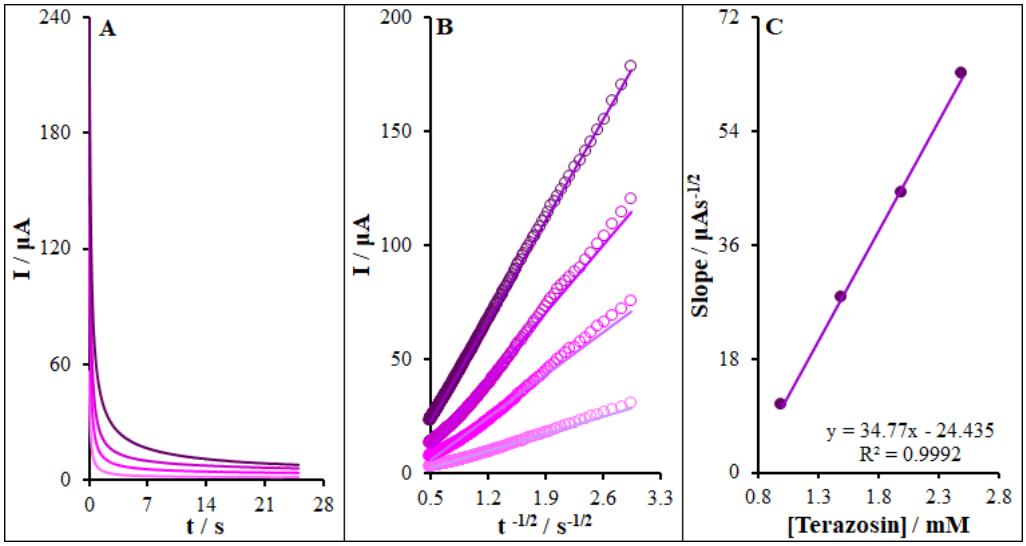

Fig. 8. (A) Chronoamperograms obtained at M-CeO_2-HS/GCE 0.1 M PBS (pH 7.0) for different concentrations of terazosin (from inner to outer curve): 1.0, 1.5, 2.0 and 2.5 mM. (B) Plots of I *vs.* $t^{-1/2}$ obtained from chronoamperograms 1-4. (C) Plot of the slope of the straight lines against terazosin concentration.

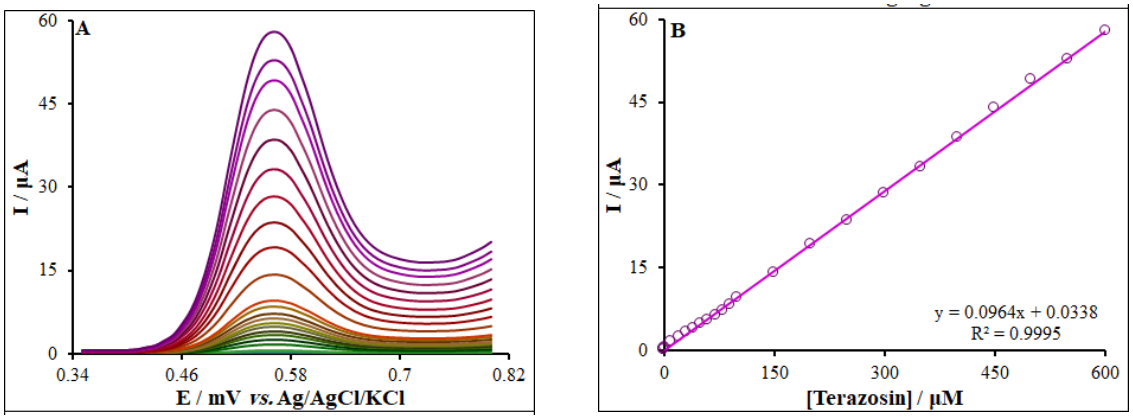

Fig. 9. (A) DPVs of M-CeO_2-HS/GCE in 0.1 M (pH 7.0) containing different concentrations of terazosin (from inner to outer curve): 0.01, 0.1, 1.0, 10.0, 20.0, 30.0, 40.0, 50.0, 60.0, 70.0, 80.0, 90.0, 100.0, 150.0, 200.0, 250.0, 300.0, 350.0, 400.0, 450.0, 500.0, 550.0 and 600.0 µM. (B) Plot of the electrocatalytic peak current as a function of terazosin concentration in the range of 0.01 to 600.0 µM, respectively.

fitted the square root of scan rate ($v^{1/2}$), according to the regression equation below:

$$Ipa\ (\mu A) = 1.0015\ v^{1/2}\ (mVs^{-1}) + 3.254\ (R^2 = 0.9996)$$

Therefore, the terazosin-electrode reactions are surface diffusion controlled reactions.

Chronoamperometric analyses

The chronoamperograms with the active electrode potential of 620 mV were applied to measure the diffusion coefficient (D) value (cm^2/s) on modified electrode surface for terazosin detection at different target concentrations, as seen in Fig. 8A. Cottrell equation (4) was used to determine electroactive species for redox current under surface diffusion controlled reactions [41]:

$$I = nFAD^{1/2}C_b\pi^{-1/2}t^{-1/2} \quad (4)$$

Where, I stand for controlling the current of terazosin diffusion from the mass solution towards the solution/ electrode interface, A for the electrode surface area (cm^2), and C for terazosin bulk concentration (mol/cm^{-3}). Based on plot of I versus $t^{-1/2}$ and the slopes, the mean D value was 1.9 $\times 10^{-6}$ cm^2/s (Fig. 8B and C).

Table 2. The application of M-CeO_2-HS/GCE for concurrent determination of terazosin in terazosin tablets, human blood serum and urine samples. All concentrations are in μM.

Sample	Spiked	Found[a]	Recovery (%)
Terazosin tablet	-	3.5±2.4	-
	5.0	8.3±3.1	97.6
	10.0	13.6±1.8	100.7
	15.0	18.4±2.6	99.4
Human blood serum	-	ND[b]	-
	5.0	5.1±3.3	102.0
	10.0	10.1±1.7	101.0
	15.0	14.7±2.1	98.0
Urine	-	ND[b]	-
	20.0	19.9±2.4	99.5
	25.0	25.3±2.9	101.2
	30.0	29.9±2.8	99.6

[a] Mean±standard deviation for n=5.
[b] Not detect

DPV measurements

Fig. 9 shows the DPV for detection of different terazosin concentrations on the surface of M-CeO_2-HS/GCE under optimal conditions (initial potential of 0.35-0.8 V, amplitude of 0.05 V, step potential of 0.01 V, and frequency of 10 Hz). A linear relationship was found between the terazosin concentration and the peak current (0.01 to 600.0 μM) under the regression equation of y = 0.0964x + 0.0338 with R^2= 0.9995 (Fig. 9). The limit of detection (LOD, $3S_b/m$) was estimated at 1.9 nM; where, S_b stands for standard deviation of blank and m for slope of calibration plot.

Table 1 shows rare reports of electrochemically terazosin detection [30-33]. The first study was conducted by Sefid-sefidehkhan et al. (2017) using voltammetry method to detect terazosin, with the LOD value of 19.0 nM [30]. Atta et al. (2007) detected the terazosin at different concentrations of 0.04 μM-2.4 μM, with the LOD value of 0.6 μM [31]. Madarekian et al. modified a carbon paste electrode (CPE) with ZnO nanoparticles and reduced graphene oxide to detect the terazosin at different concentrations of 0.01-10.0 μM using differential pulse voltammetry methodology, with the LOD value of 2.0 nM [32]. Kiranami et al. (2017) introduced a CPE modified with poly congo red to detect terazosin, with the LOD value of 7.3 μM [33]. Although these methods are accurate and reliable, there are several disadvantages to them, such as poor LOD, limited linear range and high cost. As shown in Table 1, lower LOD, acceptable linear dynamic range, and proportional or even higher sensitivity were found for our sensor, compared to other terazosin detection sensors reported in previous studies. The wonderful outcomes from the suggested sensor can be attributed to the excellent electron transfer and the high effective surface area of M-CeO_2-HS, through which high sensitivity was conducted to a synergic influence towards terazosin detection.

Reproducibility, repeatability and stability

The DPV method was used to study stability, reproducibility and repeatability of electrochemically fabricated sensor under optimized conditions. After six consecutive applications of M-CeO_2-HS/GCE to measure 10.0 μM of terazosin solution, no distinct change was found in the DPV response. The relative standard deviation (RSD%) of 0.96% confirmed satisfactory repeatability of proposed sensor. The DPV method was performed additionally to assess the electrode reproducibility. Six consecutive measurements were carried out to evaluate reproducibility, followed by calculating RSD%. The intra-electrode and inter-electrode RSD% was about 1.27% and 2.98%, respectively. The stability of the modified electrochemical sensor was analyzed as well. The electrodes were left in an ambient room for three weeks, and there was no significant fluctuation in peak current (2.7 %), confirming the appropriate stability of M-CeO_2-HS/GCE electrode under the optimized conditions. The selectivity of method

was evaluated by testing 10.0 µM terazosin solution in exposure to several compounds with potential interference containing 100-fold sucrose, ascorbic acid, citric acid, dopamine, vitamin B_6, uric acid, vitamin B_2, glucose and starch; and 20-fold amaranth and quinoline yellow. According to the results (the signal change of less than 3%), no significant interference was seen between those compounds and terazosin detection. The proposed method subsequently demonstrated a considerable selectivity for the terazosin detection.

Analytical applications

In clinical applications, the applicability of proposed sensor, M-CeO_2-HS/GCE was used to detect different terazosin concentrations in terazosin tablets and real human (urine and blood serum) samples, the results of which are shown in Table 2. The mean terazosin recovery was calculated to be 97.6-102.0 %. The RSD value of <4% confirmed the accurate suitability of this method, which met the microanalysis needs. Hence, our introduced method can be clinically applicable for the terazosin detection.

CONCLUSION

The ongoing study constructed a new electrochemical modifier to detect terazosin using M-CeO_2-HS/GCE sensor that was then characterized by many instrumental, the results of which showed better electrochemical properties compared with bare GCE because of acceptable conductivity and large electroactive area of M-CeO_2-HS. Therefore, the produced sensor possessed the electrochemical properties such as low limit of detection, simple production process, acceptable reproducibility and repeatability, great sensitivity, prolonged electrode response stability, broad linear dynamic range and cost-effectiveness in quality control, clinical analysis, and conventional drug preparations.

CONFLICT OF INTEREST

The authors declare no conflict of interest.

REFERENCES

1. A. Shrivastava, V. B. Gupta, Various treatment options for benign prostatic hyperplasia: A current update. J. Midlife. Health. 2012, 3: 10-19. https://doi.org/10.4103/0976-7800.98811
2. I. S. Shin, M.Y. Lee, H.K. Ha, C.S. Seo, H.K. Shin, Inhibitory effect of Yukmijihwang-tang, a traditional herbal formula against testosterone-induced benign prostatic hyperplasia in rats. BMC Complement. Altern. Med. 2012, 12: 1472- 6882. https://doi.org/10.1186/1472-6882-12-48
3. A. Shrivastava, Various Analytical Methods for the Determination of Terazosin in Different Matrices. World J. Anal. Chem. 2013, 1; 80-86.
4. M. Zeeb, M. Sadeghi, Sensitive Determination of Terazosin in Pharmaceutical Formulations and Biological Samples by Ionic-Liquid Microextraction Prior to Spectrofluorimetry. Inter. J. Anal. Chem. 2012, 2012: 1-7. https://doi.org/10.1155/2012/546282
5. C.C. Wang, M.O. Luconi, A.N. Masi, L. Fernandez, Determination of terazosin by cloud point extraction-fluorimetric combined methodology. Talanta 2007, 72: 1779-1785. https://doi.org/10.1016/j.talanta.2007.02.010
6. N.A. Mohamed, S. Ahmed, S.A. El Zohny, A Specific High-Performance Thin-Layer Chromatography with Fluorescence Detection for the Determination of Some a1-Blockers. J. Liq. Chromatogr. Relat. Technol. 2015, 38: 271-282. https://doi.org/10.1080/10826076.2014.903852
7. P.S. Sarsambi, G.K. Kapse, S.A. Raju, Visible Spectrophotometric Determination of Terazosin Hydrochloride from Bulk Drug and Formulations. Asian J. Chem. 2002, 14: 545-547.
8. Z. Hong-Yan, W. Hai-Long, Y. Li-Qun Ou, Z. Yan, N. Jin-Fang, F. Hai-Yan, Y. Ru-Qin, Fluorescent quantification of terazosin hydrochloride content in human plasma and tablets using second-order calibration based on both parallel factor analysis and alternating penalty trilinear decomposition. Anal. Chim. Acta 2009, 650: 143-149. https://doi.org/10.1016/j.aca.2009.07.022
9. C.C. Wang, M.O. Luconi, A.N. Masi, L. Fernandez, Determination of terazosin by cloud point extraction-fluorimetric combined methodology. Talanta 2007, 72: 1779-1785. https://doi.org/10.1016/j.talanta.2007.02.010
10. M.M. Ghoneim, M.A. El Ries, E. Hammam, A.M. Beltagi, A validated stripping voltammetric procedure for quantification of the anti-hypertensive and benign prostatic hyperplasia drug terazosin in tablets and human serum. Talanta 2004, 64: 703-710. https://doi.org/10.1016/j.talanta.2004.03.043
11. R. Ferretti, B. Gallinella, F. La Torre, L. Zanitti, L. Turchetto, A. Mosca, R. Cirilli, Direct high-performance liquid chromatography enantioseparation of terazosin on an immobilised polysaccharide-based chiral stationary phase under polar organic and reversed-phase conditions. Chromatogr. A 2009, 1216: 5385-5390. https://doi.org/10.1016/j.chroma.2009.05.034
12. P.Y. Cheah, K.H. Yuen, M.L. Liong, Improved high-performance liquid chromatographic analysis of terazosin in human plasma. J. Chromatogr. B 2000, 745: 439-443. https://doi.org/10.1016/S0378-4347(00)00313-3
13. A.P. Zavitsanos, T. Alebic-Kolbah, Enantioselective determination of terazosin in human plasma by normal phase high-performance liquid chromatography-electrospray mass spectrometry. J. Chromatogr. A 1998, 794: 45-56. https://doi.org/10.1016/S0021-9673(97)00892-3
14. M. Bakshi, T. Ojha, S. Singh, Validated specific HPLC methods for determination of prazosin, terazosin and doxazosin in the presence of degradation products formed under ICH-recommended stress conditions. J. Pharm. Biomed. Anal. 2004, 34: 19-26. https://doi.org/10.1016/j.japna.2003.08.009

15. M.M. Foroughi, Sh. Jahani, Z. Aramesh-Boroujeni, M. Vakili Fathabadi, H. Hashemipour Rafsanjani, M. Rostaminasab Dolatabad, Template-free synthesis of ZnO/Fe3O4/Carbon magnetic nanocomposite: Nanotubes with hexagonal cross sections and their electrocatalytic property for simultaneous determination of oxymorphone and heroin. Michrochem. J. 2021, 170: 106679. https://doi.org/10.1016/j.microc.2021.106679
16. N. Haghnegahdar, M. Abbasi Tarighat, D. Dastan, Curcumin-functionalized nanocomposite AgNPs/SDS/MWCNTs for electrocatalytic simultaneous determination of dopamine, uric acid, and guanine in co-existence of ascorbic acid by glassy carbon electrode. J. Mater. Sci. Mater. Electron. 2021, 32: 5602-5613. https://doi.org/10.1007/s10854-021-05282-1
17. Z. Fathi, Sh. Jahani, M. Shahidi Zandi, M.M. Foroughi, Synthesis of bifunctional cabbage flower-like Ho3+/NiO nanostructures as a modifier for simultaneous determination of methotrexate and carbamazepine. Anal. Bioanal. Chem. 2020, 412: 1011-1024. https://doi.org/10.1007/s00216-019-02326-8
18. M. Nazari, S. Kashanian, R. Mohammadi, Electrodeposition of anionic, cationic and nonionic surfactants and gold nanoparticles onto glassy carbon electrode for catechol detection. J. Nanoanal. 2019, 6: 48-56.
19. M. Vakili Fathabadi, H. Hashemipour Rafsanjani, M.M. Foroughi, Sh. Jahani, N. Arefi Nia, Synthesis of Magnetic Ordered Mesoporous Carbons (OMC) as an Electrochemical Platform for Ultrasensitive and Simultaneous Detection of Thebaine and Papaverine. J. Electrochem. Soc. 2020, 167: 027509. https://doi.org/10.1149/1945-7111/ab6446
20. M. Fathinezhad, M. Abbasi Tarighat, D. Dastan, Chemometrics heavy metal content clusters using electrochemical data of modified carbon paste electrode. Environ. Nanotechnol. Monit. Management 2020, 14: 100307. https://doi.org/10.1016/j.enmm.2020.100307
21. N. Sheibani, M. Kazemipour, Sh. Jahani, M.M. Foroughi, A novel highly sensitive thebaine sensor based on MWCNT and dandelionlike Co3O4 nanoflowers fabricated via solvothermal synthesis. Microchem. J. 2019, 149: 103980. https://doi.org/10.1016/j.microc.2019.103980
22. F. Altef, R. Batool, R. Gill, Z. Ur Rehman, H. Majeed, A. Ahmad, M. Shafiq, D. Dastan, G. Abbas, K. Jacob, Synthesis and electrochemical investigations of ABPBI grafted montmorillonite based polymer electrolyte membranes for PEMFC applications, Renew. Energy 2021, 164: 709-728. https://doi.org/10.1016/j.renene.2020.09.104
23. A. Asghar Pasban, E. Hossein Nia, M. Piryaei, Determination of Acetaminophen Via TiO2/MWCNT Modified Electrode. J. Nanoanal. 2017, 4: 142-149.
24. M.M. Foroughi, Sh. Jahani, Z. Aramesh-Boroujeni, M. Rostaminasab Dolatabad, K. Shahbazkhani, Synthesis of 3D cubic of Eu3+/Cu2O with clover-like faces nanostructures and their application as an electrochemical sensor for determination of antiretroviral drug nevirapine. Ceram. Int. 2021, 47: 19727-19736. https://doi.org/10.1016/j.ceramint.2021.03.311
25. D. Dastan, Nanostructured Anatase Titania Thin Films Prepared by Sol-Gel Dip Coating Technique, J. Atomic, Molecul., Condensate Nano Phys. 2015, 2: 109-114. https://doi.org/10.26713/jamcnp.v2i2.331
26. N. Arefi Nia, M.M. Foroughi, Sh. Jahani, Simultaneous determination of theobromine, theophylline, and caffeine using a modified electrode with petal-like MnO2 nanostructure. Talanta 2020, 222: 121563. https://doi.org/10.1016/j.talanta.2020.121563
27. D. Dastan, N.B. Chaure, Influence of surfactants on TiO2 nanoparticles grown by Sol-Gel Technique, J. Mater. Mech. Manufact. 2014, 2: 21-24. https://doi.org/10.7763/IJMMM.2014.V2.91
28. N. Jandaghi, Sh. Jahani, M.M. Foroughi, M. Kazemipour, M. Ansari, Cerium-doped flower-shaped ZnO nano-crystallites as a sensing component for simultaneous electrochemical determination of epirubicin and methotrexate. Microchim. Acta 2020, 187: 24-35. https://doi.org/10.1007/s00604-019-4016-2
29. G.L. Tan, D. Tang, D. Dastan, A. Jafari, J.P.B. Silva, X.T. Yin, Effects of Heat Treatment on Electrical and Surface Properties of Tungsten Oxide Thin Films Grown by HFCVD Technique. Mater. Sci. Semicond. Process 2021, 122: 105506. https://doi.org/10.1016/j.mssp.2020.105506
30. M.M. Foroughi, M. Noroozifar, M. Khorasani-Motlagh, Simultaneous determination of hydroquinone and catechol using a modified glassy carbon electrode by ruthenium red/carbon nanotube. J. Iran. Chem. Soc. 2015, 12: 1139-1147. https://doi.org/10.1007/s13738-014-0575-7
31. S. Kashanian, M. Nazari, R. Mohammadi, Electrodeposition of anionic, cationic and nonionic surfactants and gold nanoparticles onto glassy carbon electrode for catechol detection. J. Nanoanal. 2018. DOI: 10.22034/jna.2018.575531.1106.
32. M.M. Foroughi, M. Ranjbar, Microwave-assisted synthesis and characterization photoluminescence properties: a fast, efficient route to produce ZnO/GrO nanocrystalline. J. Mater. Sci.: Mater. Electron. 2017, 28: 1359-1363. https://doi.org/10.1007/s10854-016-5668-x
33. G.L. Tan, D. Tang, D. Dastan, A. Jafari, Z. Shi, Q.Q. Chu, J.P.B. Silva, X.T. Yin, Structures, Morphological Control, and Antibacterial Performance of Tungsten Oxide Thin Films. Ceram. Int. 2021, 47: 17153-17160. https://doi.org/10.1016/j.ceramint.2021.03.025
34. D. Yinhua, M.M. Foroughi, Z. Aramesh-Boroujeni, Sh. Jahani, M. Peydayesh, F. Borhani, M. Khatami, M. Rohani, M. Dusek, V. Eigner, The synthesis, characterization, DNA/BSA/HSA interactions, molecular modeling, antibacterial properties, and in vitro cytotoxic activities of novel parent and niosome nano-encapsulated Ho(III) complexes. RSC Adv. 2020, 10: 22891-22908. https://doi.org/10.1039/D0RA03436C
35. K. Shan, Z.Z. Yi, X.T. Yin, L. Cui, D. Dastan, Diffusion kinetics mechanism of oxygen ion in dense diffusion barrier limiting current oxygen sensors. J. Alloys Compd. 2021, 855: 157465. https://doi.org/10.1016/j.jallcom.2020.157465
36. N. Farvardin, Sh. Jahani, M. Kazemipour, M.M. Foroughi, The synthesis and characterization of 3D mesoporous CeO2 hollow spheres as a modifier for the simultaneous determination of amlodipine, hydrochlorothiazide and valsartan. Anal. Methods 2020, 12: 1767-1778. https://doi.org/10.1039/D0AY00022A
37. T. Montini, M. Melchionna, M. Monai, P. Fornasiero, Fundamentals and Catalytic Applications of CeO2-Based Materials. Chem. Rev. 2016, 116: 5987-6041. https://doi.org/10.1021/acs.chemrev.5b00603
38. X. Gong, Y.Q. Gu, N. Li, H. Zhao, C.J. Jia, Y. Du, Thermally Stable Hierarchical Nanostructures of Ultrathin MoS2

Nanosheet-Coated CeO2 Hollow Spheres as Catalyst for Ammonia Decomposition. Inorg. Chem. 2016, 55: 3992-3999. https://doi.org/10.1021/acs.inorgchem.6b00265
39. K. Shan, Z.Z. Yi, X.T. Yin, D. Dastan, S. Dadkhah, B.T. Coates, H. Garmestani, Mixed conductivities of A-site deficient Y, Cr-doubly doped SrTiO3 as novel dense diffusion barrier and temperature-independent limiting current oxygen sensors. Adv. Powder Technol. 2020, 31: 4657-4664. https://doi.org/10.1016/j.apt.2020.10.015
40. K. Shan, F. Zhai, Z.Z. Yi, X.T. Yin, D. Dastan, F. Tajabadi, A. Jafari, S. Abbasi, Mixed Conductivity and the Conduction Mechanism of the Orthorhombic CaZrO3 based Materials. Surf. Interfaces 2021, 23: 100905. https://doi.org/10.1016/j.surfin.2020.100905
41. A. Bard, L. Faulkner, Electrochemical methods fundamentals and applications. second ed., New York: Wiley, 2001.
42. Y. Sefid-sefidehkhan, K. Nekoueian, M. Amiri, M. Sillanpaa, H. Eskandari, Palladium nanoparticles in electrochemical sensing of trace terazosin in human serum and pharmaceutical preparations. Mater. Sci. Eng. C 2017, 75: 368-374. https://doi.org/10.1016/j.msec.2017.02.061
43. N.F. Atta, S.A. Darwish, S.E. Khalil, A. Galal, Effect of surfactants on the voltammetric response and determination of an antihypertensive drug. Talanta 2007, 72: 1438-1445. https://doi.org/10.1016/j.talanta.2007.01.053
44. T. Madrakian, H. Ghasemi, A. Afkhami, E. Haghshenas, ZnO/rGO nanocomposite/carbon paste electrode for determination of terazosin in human serum samples. RSC Adv. 2016, 6: 2552-2558. https://doi.org/10.1039/C5RA24367J
45. S. Kiranmai, Y.V. Manohara Reddy, M. Venu, C. Madhuri , K. Anitha, G. Madhavi, A.V. Reddy, Determination of Terazosin by using Poly (Congo red) Modified Carbon Paste Electrode. Anal. Bioanal. Electrochem. 2017, 9: 154-163.